EJAM
www.ejamjournal.com

Electronic Journal of Applied Mathematics

Research article

Mersin University Publishing
DOI: ejam.20253260
2025, Vol. 3, No. 2, 49–64

A delayed eco-epidemiological prey–predator model and its discrete analogue under the weak Allee-effect

Kalyan Das[1,*], **G.Ranjith Kumar**[2]

1. Department of Interdisciplinary Sciences National Institute of Food Technology Entrepreneurship and Management, HSIIDC Industrial Estate, Kundli, Haryana, India
2. Department of Mathematics, Anurag University, Venkatapur, Hyderabad, India

*Corresponding author

Abstract

This study looks into a delayed predator–prey model that includes competition within the hunter species and a strong Allee effect in the prey population. The time delay is used as a bifurcation measure to look at how stable the coexistence equilibrium is. Our findings show that a Hopf splitting can happen when the delay goes over a certain level. The normal for m theory and center manifold method is used to find the direction and stability of the periodic solutions that are made. Number simulations add to the evidence for the mathematical findings.

Keywords: Allee-effect, Stability, Hopf-bifurcation, Intra-specific competition
2020 Mathematics Subject Classification: 34D20, 34C23, 37J70
Article history: Received 12 Feb 2025; Accepted 1 May 2025; Online 22 Jun 2025

1 Introduction

Building on the foundational work of Lotka [1913] and Volterra [1926], numerous researchers have focused on the complex dynamical analysis of ordinary differential equations through mathematical modelling. Various two-dimensional models have been explored to underst and the interaction dynamics between prey and predator species in deterministic environments. These models are based on the classical Lotka–Volterra framework, which, despite its significance, is known to exhibit structural instability. A critical aspect in the for mulation of predator–prey models is the careful selection of the prey growth function. In this context, many researchers have investigated Gause-type prey–predator models featuring prey-dependent functional responses and logistic growth assumptions for the prey population. However, such models possess inherent limitations and can capture only a restricted range of dynamic behaviors. One important ecological phenomenon that has gained increasing attention is the

Contact: Kalyan Das daskalyan27@gmail.com; G.Ranjith Kumar ranjithreddy1982@gmail.com

© 2025 The Author(s). Published by Mersin University Press. This is an Open Access article distributed under the terms of the Creative Commons Attribution 4.0 International License, which permits unrestricted use, distribution, and reproduction in any medium, provided the original author and source are credited.

Allee effect, which has been observed in several animal populations and holds significant implications for species survival and population dynamics.

The Allee effect, first documented by W. C. Allee in 1931, describes a phenomenon in which individual fitness positively correlates with population density, particularly at low densities. This effect can result from challenges such as difficulty in mate finding, social instability in small groups, inbreeding depression, inefficient resource utilization, and reduced efficacy in predator avoidance or defense. The Allee effect is commonly categorized into two types: strong and weak (or moderate). A strong Allee effect is characterized by a critical population threshold below which the population experiences negative growth, leading potentially to extinction [22, 23]. In contrast, a moderate Allee effect slows population growth at low densities but does not reverse it; the growth rate remains positive even in small populations [24, 25, 26].

In the last few decades, many mathematical models have been developed that include Allee effects. The behaviour of these models is considerably more complex than those based on st and ard logistic growth functions [1, 2, 3, 4, 5, 6, 7, 8]. Incorporating the Allee effect into mathematical for mulations makes it possible to capture real-world ecological situations such as group for mation, predator invasion, and interspecific competition. This enhancement makes predator–prey models more realistic and useful for describing a wider range of species interactions and environmental conditions.

Importantly, the Allee effect is widely recognized as a factor that increases the risk of both local and global extinction and has profound implications for population dynamics [9, 10, 11]. In the context of predator–prey systems, the incorporation of Allee effects has proven both insightful and necessary [12, 13, 14]. At low population densities, the Allee effect introduces a positive density dependence, where the per capita growth rate increases with population density. The strength of this effect can significantly influence model outcomes: a pronounced Allee effect leads to population decline at low densities, while a weaker for m allows for population persistence albeit with slower growth.

1.1 Mathematical Model for mulation

A commonly studied predator–prey model that accounts for intra-specific competition among predators is typically represented in the following for m.

$$\begin{aligned} \frac{dx}{dt} &= xf(x,L) - yH(x), \\ \frac{dy}{dt} &= \beta yH(x) - \mu y - \theta y^2. \end{aligned} \tag{1}$$

Let x(t) and y(t) denote the population densities of the prey and predator, respectively, at time t. The parameter r represents the intrinsic growth rate per capita of the prey and L denotes the environmental carrying capacity. The parameter α is the conversion efficiency of the predator, $f(x)$ denotes the functional response, d is the natural death rate of the predator and β represents the rate of intraspecific competition between predators. This equation represents the most commonly used continuous growth function that incorporates the Allee effect.

$$\frac{dx}{dt} = rx\left(1 - \frac{x}{L}\right)(x - b) \tag{2}$$

In the above equation, the Allee effect is classified as strong when $b >$ and weak when $b \leq$. In the present study, we focus on the case of a strong Allee effect in the prey population, and thus we assume $0 < b < L$. where L is the environmental carrying capacity.

It is biologically realistic to incorporate time delay into predator–prey models, as time lags are inherent in many biological processes and are considered a key factor contributing

to periodic fluctuations in population density [15, 16, 17, 18, 19, 20, 21]. Specifically, predator reproduction does not respond instantaneously to changes in prey availability; rather, a finite period such as gestation or maturation is typically required. To reflect this, we introduce a constant time delay τ into the proposed model. As a result, the system is for mulated as a set of delay differential equations.

$$\begin{aligned} \frac{dx}{dt} &= rx\left(1-\frac{x}{L}\right)(x-b)-\beta xy, \\ \frac{dy}{dt} &= \beta x(t-\tau)y-my-\theta y^2. \end{aligned} \tag{3}$$

with the initial conditions $x(0) > 0, y(0) > 0$. In the above system, $x(t)$ and $y(t)$ represent the population densities of the prey and predator, respectively. The parameters (put all parameters) are all positive constants, where r is the intrinsic growth rate of the prey, L is the environmental carrying capacity, α is the prey capture rate, b is the survival threshold of the prey associated with the Allee effect, d is the natural death rate of the predator, and β denotes the intra-specific competition rate among predators.

We also investigate the discrete counterpart of the continuous population model under consideration. Discrete models generally exhibit more complex and richer dynamics compared to their continuous counterparts. As a result, many researchers [29, 30, 31, 32] have studied discrete models to analyze the population dynamics of predator–prey interactions. Such models are typically for mulated using difference equations, which also facilitate straight for ward numerical simulations.

The remainder of the paper is organized as follows: Section 2 addresses the positivity and boundedness of the proposed mathematical model. Section 3 investigates the existence of equilibrium points and analyzes their local asymptotic stability. In Section 4, we study the Hopf bifurcation of the model. Section 5 applies the normal for m theory and center manifold theorem to determine the direction and stability of bifurcating periodic solutions. Section 6 introduces the discrete variant of the model, including its equilibrium points, stability analysis, and bifurcation behavior. Numerical simulations supporting our theoretical results are presented in Section 7 . Finally, in Section 8 concludes the paper with discussion and summary of the main findings.

2 Dynamics of the model of system (2)

for $\tau = 0$ the system (3) can be reduced to the for m

$$\begin{aligned} \frac{dx}{dt} &= rx\left(1-\frac{x}{L}\right)(x-b)-\beta xy, \\ \frac{dy}{dt} &= \beta xy-my-\theta y^2. \end{aligned} \tag{4}$$

2.1 Positivity of solution

The following theorems establish the positivity and boundedness of the system's solutions. **Theorem:2.1** for system (4). all solutions $(x(t), y(t))$ with a non-negative initial condition $(x(0), y(0))$ remain nonnegative for all $t \geq 0$ and are ultimately bounded. This follows from st and ard results on the invariance of the non-negative and boundedness of solutions in biological systems (see [33, 34]).

2.2 Boundedness of solution

Theorem 2.1. *The solutions of the system (4) are bounded.*

Proof. Let $z = x + y$

$$\begin{aligned}\frac{dz}{dt} &= \frac{dx}{dt} + \frac{dy}{dt} \\ &= rx\left(1 - \frac{x}{L}\right)(x - b) - my - \theta y^2 \\ &\leq rx^2\left(1 + \frac{b}{L}\right) - my \leq rx\end{aligned}$$

Let us consider $(x(t), y(t))$ to be an arbitrary positive solution of the system (4) subject to a positive initial condition. From equation one of system (4)

$$x(t) = x(0)\exp\left[\int_0^t L\left(x(p), y(p)\right)dp\right]$$

where

$$L\left(x(p), y(p)\right) = rx(p)\left(1 - \frac{x(p)}{L}\right)(x(p) - b) - \beta x(p)y(p).$$

Case (i): Consider $x(0) \leq 1$ and our claim is $x(t) \leq 1$, for all $t \geq 0$. Otherwise there exist two positive real numbers t_1 and t_2 such that $x(t_1) = 1$ and $x(t) > 1$, for all $t \in (t_1, t_2)$.

$$\begin{aligned}x(t) &= x(0)\exp\left[\int_0^t L\left(x(p), y(p)\right)dp\right] \\ &= x(0)\exp\left[\int_0^{t_1} L\left(x(p), y(p)\right)dp\right] \times \exp\left[\int_{t_1}^t L\left(x(p), y(p)\right)dp\right] \triangleright \\ &= x(t_1)\exp\left[\int_{t_1}^t F\left(x(p), y(p)\right)dp\right] < x(t_1)\end{aligned}$$

as $F\left(x(p), y(p)\right) < 0$ for all $t \in (t_1, t_2)$ which contradicts our hypothesis. Hence, $x(t) \geq 1$.

Case (ii): Next, we consider $x(0) > 1$. Then as long as $x(t) \geq 1$

$$x(t) = x(0)\exp\left[\int_0^t L\left(x(p), y(p)\right)dp\right] < x(0)$$

as $F\left(x(p), y(p)\right) < 0$ for $x(t) \geq 1$. Hence, combining case (i) and case (ii), we can say that any positive solution satisfies $x(t) \leq \max\{x(0), 1\}$. for $t \geq 0$.

Also, from the second equation in (4), we have $\frac{dy}{dt} \leq y\left(\beta - m - \theta\right)$ which clearly implies that $\lim_{t\to\infty} \sup y\left(t\right) \leq \frac{\beta - m}{\theta} \simeq \delta_1$.

As solutions of the model are always positive, we must have the parametric restriction $\beta > m$. Hence, we have the theorem. □

3 Existence of equilibrium points

Equilibrium points are the intersection points of the equations in system (4). Here we can have three different equilibrium points trivial, axial and interior equilibrium points.

(i) Trivial equilibrium point: $E_0 = (0, 0)$

(ii) Axial equilibrium point: First axial equilibrium point $E_1 = (b, 0)$ and Second axial equilibrium point $E_2 = (L, 0)$

(iii) Interior equilibrium point: $E^* = (x^*, y^*)$ where

$$x^* = \frac{L}{2r\theta}\left\{\left[r\theta\left(1+\frac{b}{L}\right)-\beta^2\right]+\sqrt{\left(\beta^2 - r\theta - \frac{r\theta b}{L}\right)^2 - \frac{4r\theta}{L}\left(r\theta b - m\beta\right)}\right\}$$

and

$$y^* = \frac{r}{\beta}\left[x^*\left(1-\frac{x^*}{L}+\frac{b}{L}\right)-b\right].$$

The interior equilibrium point exists if

$$\begin{aligned} &\frac{r\theta b}{m} < \beta < \sqrt{r\theta\left(1+\frac{b}{L}\right)}, \\ &x^*\left(1-\frac{x^*}{L}+\frac{b}{L}\right) > b. \end{aligned} \tag{5}$$

In ecology, emphasis is placed on the stability of the coexisting equilibrium. Therefore, we investigate the local stability of the positive equilibrium of system (4).

4 Local stability analysis with Hopf-bifurcation

The Jacobian matrix of the system (3) at interior equilibrium point is given by

$$J = \begin{bmatrix} -\frac{rx^*}{L}\left(b - 2x^* + L\right) & \beta x^* \\ \beta e^{-\lambda\tau} y^* & -\theta y^* \end{bmatrix} \tag{6}$$

The characteristic equation of (5) is given by

$$\lambda^2 + M_1\lambda + M_2 + e^{-\lambda\tau}N_1 = 0 \tag{7}$$

where $M_1 = \theta y^* - \frac{rx^*}{L}\left(b - 2x^* + L\right); M_2 = \frac{-\theta y^* r x^*}{L}\left(b - 2x^* + L\right); N_1 = \beta^2 x^* y^*$.

In absence of the time delay i.e., $\tau = 0$ (6) reduces to $\lambda^2 + M_1\lambda + M_2 = 0$. The interior equilibrium point is locally asymptotically stable if $M_1 > 0$ and $M_2 > 0$ (by Routh-Hurwitz criteria).

$$\begin{aligned} M_1 > 0 \quad &\text{if} \quad \frac{rx^*(b+L)}{2r(x^*)^2 + L\theta y^*} < 1, \\ M_2 > 0 \quad &\text{if} \quad \beta > \sqrt{\tfrac{r\theta}{L}\left(b + L - 2x^*\right)}. \end{aligned} \tag{8}$$

Theorem 4.1. *The positive equilibrium of system (4) is locally asymptotically stable if* $\frac{rx^*(b+L)}{2rx^{*2}+L\theta y^*} < 1$ *and* $\beta > \sqrt{\frac{r\theta}{L}\left(b + L - 2x^*\right)}$.

Theorem 4.2. *Hopf-bifurcation occurs in system (3) at the endemic equilibrium point when* $\tau = \tau_0$.

Proof. Substituting $\lambda = i\omega$ into (6) gives

$$-\omega^2 + M_2 + N_1 \cos\omega\tau + i\left(M_1\omega - N_1 \sin\omega\tau\right) = 0$$

Comparing real and imaginary parts, we get

$$\begin{aligned} N_1\cos(\omega\tau) - \omega^2 + M_2 &= 0, \\ M_1\omega - N_1\sin(\omega\tau) &= 0. \end{aligned} \tag{9}$$

squaring and adding above two equations

$$\omega^4 + B_1\omega^2 + B_2 = 0 \tag{10}$$

where $B_1 = M_1^2 - 2M_2$ and $B_2 = M_2^2 - N_1^2$.

The above equation has at most one positive root if $B_1 > 0$ and $B_2 < 0$. If the criteria mentioned above are satisfied, then equation (10) has a unique positive root and we have, $\tau_z = \frac{1}{\omega_0}\cos^{-1}\left[\frac{\omega^2 - M_2}{N_1}\right] + \frac{2z\pi}{\omega_0}, z = 0, 1, 2, \ldots$

Next, we have to show that the system (3) go through Hopf-bifurcation at endemic equilibrium when $\tau = \tau_0$. Differentiating (7) with respect to τ. we get

$$\left(\frac{d\lambda}{d\tau}\right)^{-1} = \frac{(2\lambda + M_1) - N_1\tau e^{-\lambda\tau}}{N_1\lambda e^{-\lambda\tau}}$$

then

$$\left(\frac{d\lambda}{d\tau}\right)^{-1} = \frac{(2\lambda + M_1) - N_1\tau e^{-\lambda\tau}}{N_1\lambda e^{-\lambda\tau}} - \frac{\tau}{\lambda}.$$

Substituting $\lambda = i\omega_0$ and from (9), we get

$$\mathrm{Re}\left(\left(\frac{d\lambda}{d\tau}\right)^{-1}\Bigg|_{\lambda = i\omega_0}\right) = \frac{2\omega_0^2 + \left(M_1^2 - 2M_2\right)}{M_1\omega_0^2 + \left(\omega_0^2 - M_2\right)^2} > 0 \tag{11}$$

if $M_1^2 - 2M_2 > 0$. Hence the system (3) go through the Hopf-bifurcation at endemic equilibrium when $\tau = \tau_0$. □

5 Direction and Stability of Periodic Solutions

In this section, we study the direction, stability and period of the bifurcating periodic solutions of system (3), which are generated from the positive equilibrium when $\tau = \tau^*$. The method employed is based on the normal for m theory and the center manifold theorem as introduced by Hassard et al. [27]. Let $\tau = \tau_0 + \mu.\mu \in \mathbb{R}$. $x_1 = x - x^*, x_2 = y - y^*$. $x_i = x_i(\tau t)$ then the system (3) trans for med into FDE and $u(t) = (u_1, u_2)^T \in C\left([-1, 0], R^2\right)$ as

$$\dot{u}(t) = L_\mu(u_t) + f(\mu, u_t) \tag{12}$$

where $L_\mu(\phi) = (\tau_0 + \mu)A'\phi(0) + B'\phi(-1)$ and $\phi(\theta) = (\phi_1(\theta), \phi_2(\theta))^T \in C$ where

$$A' = \begin{bmatrix} \frac{rx^*}{L}(b - 2x^* + L) & -(m + \theta y^*) \\ 0 & -\theta y^* \end{bmatrix}, \quad B' = \begin{bmatrix} 0 & 0 \\ r\left(1 - \frac{x^*}{L}\right)(x^* - b) & 0 \end{bmatrix}. \tag{13}$$

and

$$\begin{aligned} F_1 &= \alpha_{21}\phi_1^2(0) + \alpha_{22}\phi_1(0)\phi_2(0) + \alpha_{23}\phi_1^3(0), \\ F_2 &= \beta_{21}\phi_1(-1)\phi_2(0) + \beta_{22}\phi_2^2(0). \end{aligned} \tag{14}$$

where $\alpha_{21} = r + \frac{rb}{L}; \alpha_{22} = -\beta; \alpha_{23} = -\frac{r}{L}; \beta_{21} = \beta; \beta_{22} = -\theta.$

The Riesz representation theorem says that there is a function $\eta(\vartheta.\mu)$ with limited change for $\vartheta \in [-1, 0]$, such that

$$L_\mu(\phi) = \int_{-1}^{0} d\eta(\vartheta.0)\,\phi(\vartheta)$$

for $\phi \in C$. In fact, we can choose

$$\eta(\vartheta.\mu) = (\tau + \mu)\begin{pmatrix} \frac{rx^*}{L}(b - 2x^* + L) & -(m + \theta y^*) \\ 0 & -\theta y^* \end{pmatrix}\delta(\vartheta) \tag{15}$$

$$-(\overline{\tau} + \mu)\begin{pmatrix} 0 & 0 \\ r\left(1 - \frac{x^*}{L}\right)(x^* - b) & 0 \end{pmatrix}\delta(\vartheta + 1) \tag{16}$$

where δ is the Dirac delta function and $\overline{\tau}$ is a critical value of the time. for $\phi \in C'([-1, 0], R^2)$, define

$$A(\mu)\phi = \begin{cases} \frac{d\phi(\vartheta)}{d\vartheta}, & \vartheta \in [-1, 0), \\ \int_{-1}^{0} d\eta(\mu, s)\phi(s), & \vartheta = 0. \end{cases} \tag{17}$$

$$R(\mu)\phi = \begin{cases} 0, & \vartheta \in [-1, 0), \\ f(\mu, \phi), & \vartheta = 0. \end{cases} \tag{18}$$

Then the system (12) can be trans for med into the following operator equation

$$\dot{u}(t) = A(\mu)u_t + R(\mu)u_t \tag{19}$$

$$Define A^*(\psi) = \begin{cases} -\frac{d\psi(s)}{ds}, & s \in (0, 1], \\ \int_{-1}^{0} d\eta^T(t, 0)\psi(-t), & s = 0. \end{cases} \tag{20}$$

and a bilinear for m is given by

$$\langle \psi(s), \phi(\vartheta)\rangle = \overline{\psi}(0)\phi(0) - \int_{-1}^{0}\int_{0}^{\vartheta} \overline{\psi}(\xi - \vartheta)d\eta(\vartheta)\phi(\xi)d\xi \tag{21}$$

where $x(\vartheta) = \eta(\vartheta.0)$. Then $A(0)$ and A^* are adjoint operators. We first need to compute the eigen vectors of $A(0)$ and A^* corresponding to $i\overline{\omega\tau}$ and $-i\overline{\omega\tau}$, respectively. Suppose that $q(\vartheta) = (1, h)^T e^{i\overline{\omega\tau}\vartheta}$ is the eigen vector of $A(0)$ corresponding to $i\overline{\omega\tau}$ and $q^*(s) = D(1, h^*)^T e^{i\overline{\omega\tau}s}$ is the eigenvector of A^* corresponding to $-i\overline{\omega\tau}$. By a direct computation, we have

$$h = \frac{r\left(1 - \frac{x^*}{L}\right)(x^* - b)\,e^{-i\overline{\omega\tau}}}{(i\overline{\omega} + \theta y^*)}$$

and

$$h^* = \frac{-\left[\frac{rx^*}{L}\left(b-2x^*+L\right)-i\overline{\omega\tau}\right]e^{-i\overline{\omega\tau}}}{r\left(1-\frac{x^*}{L}\right)\left(x^*-b\right)}$$

From (21), we obtain $\overline{D} = \left[1+h\bar{h}^*+\overline{h}^*\overline{\tau}\left(r\left(1-\frac{x^*}{L}\right)\left(x^*-b\right)\right)e^{-i\overline{\omega\tau}}\right]^{-1}$ such that $\langle h^*, h\rangle = 1, \langle h^*, \bar{h}\rangle = 0$. Following the algorithm given in [27] and the computational process outlined in [28], we obtain the coefficients required to determine the properties of the Hopf-bifurcation.

$$g_{20} = 2\overline{\tau}\overline{D}\left\{\alpha_{21}+\alpha_{22}h^{(1)}(0)\,h^{(2)}(0)+\overline{h}^*\left[\beta_{21}h^{(1)}(-1)\,h^{(2)}(0)+\beta_{22}\left(h^{(2)}(0)\right)^2\right]\right\},$$

$$\begin{aligned} g_{11} =& \overline{\tau}\overline{D}\left\{2\alpha_{21}+\alpha_{22}\left(h^{(1)}(0)\,\bar{h}^{(2)}(0)+\bar{h}^{(1)}(0)\,h^{(2)}(0)\right)\right. && (22)\\ &\left.+\overline{h}^*\left[\beta_{21}\left(h^{(1)}(-1)\,\bar{h}^{(2)}(0)+\bar{h}^{(1)}(-1)\,h^{(2)}(0)\right)+2\beta_{22}h^{(2)}(0)\,\bar{h}^{(2)}(0)\right]\right\}, && (23)\end{aligned}$$

$$g_{02} = 2\overline{\tau}\overline{D}\left\{\alpha_{21}+\alpha_{22}\bar{h}^{(1)}(0)\,\bar{h}^{(2)}(0)+\overline{h}^*\left(\beta_{21}\bar{h}^{(1)}(0)\,\bar{h}^{(2)}(0)+\beta_{22}\left(\bar{h}^{(2)}(0)\right)^2\right)\right\},$$

$$\begin{aligned} g_{21} =& 2\overline{\tau}\overline{D}\Big\{\alpha_{21}\left(2W_{11}^1(0)+W_{20}^1(0)\right)\\ &+\alpha_{22}\Big(W_{11}^1(0)h^{(2)}(0)+\tfrac{1}{2}W_{20}^1(0)\overline{h}^{(2)}(0)+W_{11}^2(0)h^{(1)}(0)+\tfrac{1}{2}W_{20}^2(0)\overline{h}^{(1)}(0)\Big)\\ &+3\alpha_{23}\left(h^{(2)}(0)\right)^2\overline{h}^{(2)}(0)\\ &+\overline{h}^*\Big(\beta_{21}\big(W_{11}^1(-1)h^{(2)}(0)+\tfrac{1}{2}W_{20}^1(0)\overline{h}^{(2)}(0)+W_{11}^2(0)h^{(1)}(-1)+\tfrac{1}{2}W_{20}^2(0)\overline{h}^{(1)}(-1)\big)\Big)\\ &+\beta_{22}\Big(2W_{11}^2(0)h^{(1)}(0)+W_{20}^2(0)\overline{h}^{(2)}(0)\Big)\Big\}. \end{aligned} \quad (24)$$

$$W_{20}(\vartheta) = \frac{ig_{20}}{\overline{\omega\tau}}q(0)e^{i\overline{\omega\tau}\vartheta}+\frac{i\overline{g}_{02}}{3\overline{\omega\tau}}\overline{q}(0)e^{-i\overline{\omega\tau}\vartheta}+E_1e^{2i\overline{\omega\tau}\vartheta}. \quad (25)$$

$$W_{11}(\vartheta) = -\frac{ig_{11}}{\overline{\omega\tau}}q(0)e^{i\overline{\omega\tau}\vartheta}+\frac{i\overline{g}_{11}}{\overline{\omega\tau}}\overline{q}(0)e^{-i\overline{\omega\tau}\vartheta}+E_2. \quad (26)$$

$$\begin{pmatrix} 2i\overline{\omega}-\frac{rx^*}{L}\left(b-2x^*+L\right) & -\left(m+\theta y^*\right)\\ -r\left(1-\frac{x^*}{L}\right)\left(x^*-b\right)e^{-2i\overline{\omega\tau}} & 2i\overline{\omega}+\theta y^*\end{pmatrix}E_1 = 2\begin{pmatrix}E_1^{(1)}\\E_1^{(2)}\end{pmatrix}$$

$$\begin{pmatrix} \frac{rx^*}{L}\left(b-2x^*+L\right) & -\left(m+\theta y^*\right)\\ r\left(1-\frac{x^*}{L}\right)\left(x^*-b\right)e^{-2i\overline{\omega\tau}} & -\theta y^*\end{pmatrix}E_2 = -\begin{pmatrix}E_2^{(1)}\\E_2^{(2)}\end{pmatrix}$$

where

$$E_1^{(1)} = \alpha_{21}+\alpha_{22}h^{(1)}(0)\,h^{(2)}(0),$$

$$E_1^{(2)} = \beta_{21}h^{(1)}(-1)\,h^{(2)}(-1)+\beta_{22}\left(h^{(2)}(-1)\right)^2,$$

$$E_2^{(1)} = 2\alpha_{21}+\alpha_{22}\left(h^{(1)}(0)\,\bar{h}^{(2)}(0)+\bar{h}^{(1)}(0)\,\bar{h}^{(2)}(0)\right),$$

$$E_2^{(2} = \beta_{21}\left(h^{(1)}(-1)\,\bar{h}^{(2)}(-1) + \bar{h}^{(1)}(-1)\,h^{(2)}(-1)\right) \tag{27}$$

$$+ 2\beta_{22}\bar{h}^{(2)}(-1)\,\bar{h}^{(2)}(-1), \tag{28}$$

Thus, we can determine $W_{20}(\vartheta)$ and $W_{11}(\vartheta)$ from (25) and (26). Furthermore, g_{21} expression in (24) can be represented in terms of the system parameters and the constant delay. Thus, we can compute the following values:

$$C_1(0) = \frac{i}{2\bar{\omega}\bar{\tau}}\left(g_{20}g_{11} - 2|g_{11}|^2 - \frac{|g_{02}|^2}{3}\right) + \frac{g_{21}}{2},$$

$$\mu_2 = -\frac{\mathrm{Re}\{C_1(0)\}}{\mathrm{Re}\{\lambda'(\tau)\}},$$

$$\beta_2 = 2\,\mathrm{Re}\{C_1(0)\},$$

$$T_2 = -\frac{\mathrm{Im}\{C_1(0)\} + \mu_2\,\mathrm{Im}\{\lambda'(\bar{\tau})\}}{\bar{\omega}\bar{\tau}},$$

which determine the properties of the bifurcating periodic solutions on the center manifold at the critical value $\bar{\tau}$.

Theorem 5.1. *μ_2 determines the direction of the Hopf-bifurcation. If $\mu_2 > 0 (\mu_2 < 0)$. then the Hopf-bifurcation is supercritical (subcritical) and the bifurcating periodic solutions exist for $\tau > \overline{\tau}\,(\tau < \overline{\tau})$. h determines the stability of the bifurcating periodic solutions: the bifurcating periodic solutions are stable (unstable) if $h < 0\,(h > 0)$ .T_2 determines the periodic of the bifurcating periodic solution: the periodic increases (decreases) if $T_2 > 0\,(T_2 < 0)$.*

6 Discrete mathematical model for mulation

This section examines the Allee effect and intra-specific predator rivalry in the discrete predator-prey model, which is represented by the system of difference equations below.

$$\begin{aligned} x_{n+1} &= x_n + rx_n\left(1 - \tfrac{x_n}{L}\right)(x_n - b) - \beta x_n y_n, \\ y_{n+1} &= y_n + \beta x_n y_n - m y_n - \theta y_n^2. \end{aligned} \tag{29}$$

The population biomasses of the predator and prey generations n and n+1, respectively, are denoted by x and y. All of the parameters in system (29) are identical to those in system (4). Equation (29) yields a map of the plane that is not invertible. We may learn about the long-term behaviour of the predator-prey populations by examining the dynamical characteristics of the map above. The interaction of (29) generates a trajectory of the population output states in the following manner, starting from the initial condition (x_0, y_0) :
$[x(n), y(n)] = T^n[x_0, y_0]$ where $n = 0, 1, 2, \ldots$

6.1 Analysis of stability and fixed points

There are two fixed points E_1 and E_2 in system (29) that is identical to those in the continuous model (4). The stability of these fixed locations must next be examined. We review the following lemma [35, 36] in order to examine the stability of the system's fixed points (6.1).

Lemma 6.1. *Let $\phi(\lambda) = \lambda^2 - L_1\lambda + L_2$ and $\phi(1) > 0$. Let λ_1, λ_2 are two roots of $\phi(\lambda) = 0$. Then:*

(i) $|\lambda_1| < 1$ *and* $|\lambda_2| < 1$ *if and only if* $\phi(-1) > 0$ *and* $\phi(0) < 1$

(ii) $|\lambda_1| < 1$ *and* $|\lambda_2| > 1$ *if and only if* $\phi(-1) < 0$

(iii) $|\lambda_1| > 1$ *and* $|\lambda_2| > 1$ *if and only if* $\phi(-1) > 0$ *and* $\phi(0) > 1$

(iv) $\lambda_1 = -1$ *and* $\lambda_2 \neq 1$ *if and only if* $\phi(-1) = 0$ *and* $L_1 \neq 0, 2$;

(v) λ_1, λ_2 *are complex and* $|\lambda_1| = 1, |\lambda_2| = 1$ *if and only if* ${L_1}^2 - 4L_2 < 0$ *and* $\phi(0) = 1$

A fixed point (x^*, y^*) is called a sink if $|\lambda_1| < 1$ and $|\lambda_2| < 1$. So it is locally asymptotically stable. (x^*, y^*) is called a source if $|\lambda_1| > 1$ and $|\lambda_2| > 1$. so it is locally unstable. If (x^*, y^*) is called a saddle if $|\lambda_1| < 1$ and $|\lambda_2| > 1$ and (x^*, y^*) is called a non-hyperbolic if $|\lambda_1| = 1, |\lambda_2| = 1$.

By using above lemma next we can discuss the stability of auxiliary equilibrium points and positive equilibrium point.

Theorem 6.2. *Suppose that the auxiliary equilibrium point E_1*

(i) first auxiliary equilibrium point is a sink if $r < \frac{L}{b(L-b)}$ and $\beta < \frac{1+m}{b}$ and second Auxiliary equilibrium point is a sink if $r < \frac{1}{b-L}$ and $\beta < \frac{1+m}{L}$.

(ii) first auxiliary equilibrium point is a source if $r > \frac{L}{b(L-b)}$ and $\beta > \frac{1+m}{b}$ and second Auxiliary equilibrium point is a source if $r > \frac{1}{b-L}$ and $\beta > \frac{1+m}{L}$.

(iii) first auxiliary equilibrium point is a saddle if $r < \frac{L}{b(L-b)}$ and $\beta > \frac{1+m}{b}$ and second auxiliary equilibrium point is a saddle if $r < \frac{1}{b-L}$ and $\beta > \frac{1+m}{L}$.

(iv) first auxiliary equilibrium point is non-hyperbolic if $r = \frac{L}{b(L-b)}$ and $\beta = \frac{1+m}{b}$ and second auxiliary equilibrium point is a saddle if $r = \frac{1}{b-L}$ and $\beta = \frac{1+m}{L}$.

Proof. We must first calculate the system's variation matrix in order to demonstrate each of these findings. (22) at E_1 is $J_{E_1} = \begin{bmatrix} \frac{-rx^*}{L}(b - 2x^* + L) & \beta x^* \\ 0 & \beta x^* - m \end{bmatrix}$
The eigen values of above Jacobian matrix are $\lambda_1 = \frac{-rx^*}{L}(b - 2x^* + L), \lambda_2 = \beta x^* - m$.
By using Lemma 6.1 we can easily verify that Theorem 4.2 conditions at two different auxiliary equilibrium points. □

6.2 Local stability and Hopf-bifurcation

Next, we look at whether positive equilibrium (x^*, y^*) is stable locally. At the positive equilibrium (x^*, y^*). The variation matrix is

$$J_{E_2} = \begin{bmatrix} \frac{-rx^*}{L}(b - 2x^* + L) & \beta x^* \\ \beta y^* & -\theta y^* \end{bmatrix}$$

The characteristic equation of this Jacobian matrix is $\phi(\lambda) = \lambda^2 - B\lambda + C = 0$. Where $B = \frac{-rx^*}{L}(b - 2x^* + L) - \theta y^*$ and $C = \frac{r\theta x^* y^*}{L}(b - 2x^* + L) - \beta^2 x^* y^*$

Theorem 6.3. *If* $(1 + \theta y^*)\left(1 + rx^* + \frac{rx^*}{L}\right) > x^*\left(\frac{2rx^*}{K}(1 + \theta y^*) + \beta^2 y^*\right)$ *and* $\frac{2r{x^*}^2}{L} + \frac{r\theta b x^* y^*}{L} + r\theta x^* y^* - 1 > \frac{-rbx^*}{L} + rx^* + \theta y^* + \frac{2r\theta {x^*}^2 y^*}{L} + \beta^2 x^* y^* - 2$ *then the fixed point E_2 is locally asymptotically stable.*

Proof. To demonstrate that E_2 is locally stable using Lemma1, we must confirm $\phi(1) > 0, \phi(-1) > 0$ and $C < 1$.

$$\phi(1) = (1+\theta y^*)\left(1 + rx^* + \frac{rx^*}{L}\right) - x^*\left(\frac{2rx^*}{K}(1+\theta y^*) + \beta^2 y^*\right)$$

If

$$(1+\theta y^*)\left(1 + rx^* + \frac{rx^*}{L}\right) > x^*\left(\frac{2rx^*}{K}(1+\theta y^*) + \beta^2 y^*\right)$$

then $\phi(1) > 0$

$$\phi(-1) = 1 + \frac{2rx^{*2}}{L} + \frac{r\theta b x^* y^*}{L} + r\theta x^* y^* - \frac{-rbx^*}{L} - rx^* - \theta y^* - \frac{2r\theta x^{*2} y^*}{L} - \beta^2 x^* y^*$$

If

$$\frac{2rx^{*2}}{L} + \frac{r\theta b x^* y^*}{L} + r\theta x^* y^* - 1 > \frac{-rbx^*}{L} + rx^* + \theta y^* + \frac{2r\theta x^{*2} y^*}{L} + \beta^2 x^* y^* - 2$$

then $\phi(-1) > 0$

$$C < 1 => 1 - \frac{r\theta b x^* y^*}{L} + \frac{2r\theta x^{*2} y^*}{L} - r\theta x^* y^* + \beta^2 x^* y^* > 0$$

Which is true if $x^*\left(\frac{2rx^*}{K}(1+\theta y^*) + \beta^2 y^*\right) > \frac{2rx^{*2}}{L} + \frac{r\theta b x^* y^*}{L} + r\theta x^* y^* - 1$. From above results E_2 is locally asymptotically stable. □

Corollary 6.4. *The fixed point E_2 is unstable if and only if the following conditions holds*

$$x^*\left(\frac{2rx^*}{K}(1+\theta y^*) + \beta^2 y^*\right) < \frac{2rx^{*2}}{L} + \frac{r\theta b x^* y^*}{L} + r\theta x^* y^* - 1$$

or

$$\frac{2rx^{*2}}{L} + \frac{r\theta b x^* y^*}{L} + r\theta x^* y^* - 1 < \frac{-rbx^*}{L} + rx^* + \theta y^* + \frac{2r\theta x^{*2} y^*}{L} + \beta^2 x^* y^* - 2.$$

Corollary 6.5. *Suppose that*

$$\frac{2rx^{*2}}{L} + \frac{r\theta b x^* y^*}{L} + r\theta x^* y^* - 1 > \frac{-rbx^*}{L} + rx^* + \theta y^* + \frac{2r\theta x^{*2} y^*}{L} + \beta^2 x^* y^* - 2$$

then the system (29) undergoes a Hopf-bifurcation when β passes through a critical value β_c where $\det j = 1$ *at* $\beta = \beta_c$.

7 Numerical Simulation

In this part, we show several MATLAB simulations that we ran to check the accuracy of the system's analytical results for systems (3), (4) and (29).

Example 7.1. for numerical simulation for delayed model (3), we choose parameter values as $r = 1.6; L = 15.2; b = 0.052; \beta = 0.803; \mu = 0.26; \theta = 0.657$; Clearly, the interior equilibrium points for system (3) are stable for $\tau < \tau_0 = 0.12$. The stable solution converges to the positive equilibrium point. and the Hopf-bifurcating periodic solution is illustrated in Figure 1 and Figure 2 $\tau < \tau_0$ and $\tau > \tau_0$.

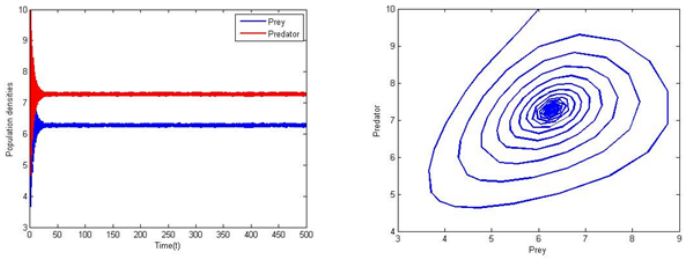

Figure 1: Time series and phase portrait of the delayed predator-prey system (3) for $\tau < \tau_0 = 0.12$ illustrating the stability of the interior equilibrium. The solution converges to a steady state, indicating that the equilibrium is locally asymptotically stable for subcritical delay values. The trajectories in the phase portrait approach the equilibrium point, and the time series shows damped oscillations converging to the steady state.

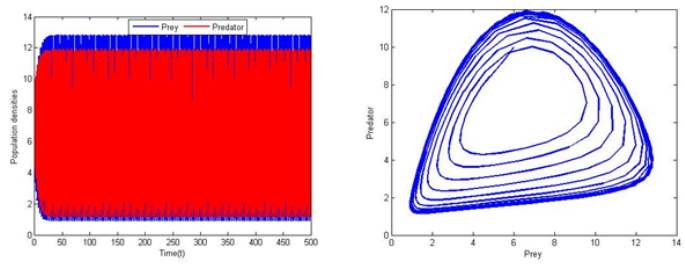

Figure 2: Time series and phase portrait of the delayed predator-prey system (3) for $\tau > \tau_0 = 0.12$. illustrating the emergence of sustained oscillations due to a Hopf bifurcation. The time series shows persistent periodic behavior in both prey and predator populations, and the phase portrait reveals a stable limit cycle around the interior equilibrium. This indicates that the equilibrium has become unstable, giving rise to oscillatory dynamics characteristic of predator-prey cycles.

Example 7.2. In this example, we explored the influence of a strong Allee effect in model (3) by taking the parameter values as follows: $r = 1.6, L = 15.2, \beta = 0.95, \mu = 0.919, \theta = 0.657$, and we discovered that with the increase of the parameter b in the model of system (4),the population gradually becomes stable with the increase of time as shown in Figure 3, while in Figure 4 is a periodic change.

Example 7.3. We now explore the dynamics of the discrete system through simulations. At first, we demonstrate the stability of system with prey-dominance. for this we chose the parameter values to be: $r = 0.06, L = 15, b = 0.152, \beta = 0.0503, m = 0.26$ and $\theta = 0.0657$. The corresponding time series values and phase plane trajectories are shown in Figure 5. Next, the predator-dominance case is depicted in Figure 6. The parameter values chosen to depict this scenario are $r = 0.206, L = 15, b = 0.00152, \beta = 0.03, m = 0.16$ and $\theta = 0.00357$. The existence of limit cycle for the parameter set $r = 0.06, L = 15, b = 0.152, \beta = 0.0803, m = 0.26$, and $\theta = 0.0657$ is depicted in Figure 7. The change in the parameter b, the survival threshold of prey from 0.152 to 0.0152. it leads to stabilization of the system, which is illustrated in Figure 8. Finally, Figure 9 presents the chaotic behavior of the system for a specific set of parameter values: $r = 0.206, L = 15, b = 0.032, \beta = 0.0027, m = 0.03$ and $\theta = 0.0017$.

8 Discussion and Concluding remarks

This paper develops a predator–prey model incorporating a strong Allee effect in the prey population and investigates its boundedness and stability properties. We extend the model by introducing a discrete time delay, resulting in an exp and ed system (denoted as model (3),

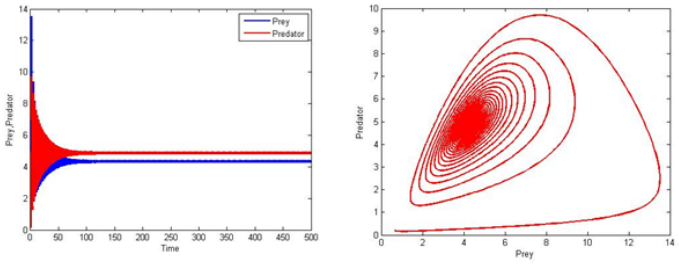

Figure 3: A time series and phase portrait of the system (4) with the Allee effect $b = 0.29$. Time series and phase portrait of system (3), illustrating the influence of a strong Allee effect in the prey population.

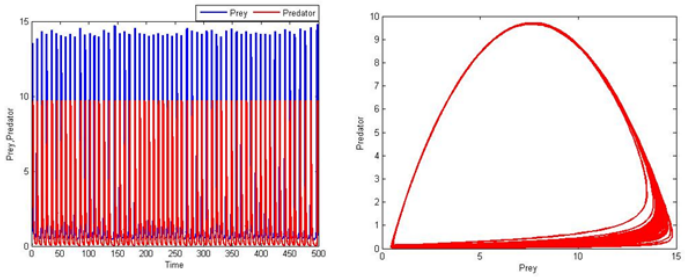

Figure 4: A time series and phase portrait of the system (4) with the Allee effect $b = 0.4$. The dynamics illustrate how the Allee effect influences population persistence: prey growth is limited below a critical threshold, impacting coexistence with predators.

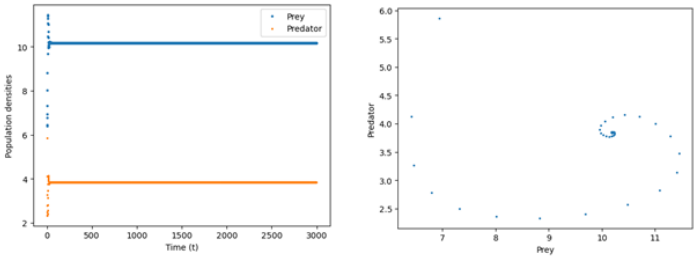

Figure 5: Simulation illustrating the stability behavior of the system (29) with prey dominance.

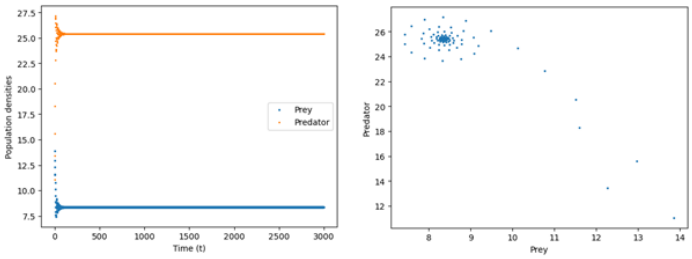

Figure 6: Simulation illustrating the stability behavior of the system (29) with predator dominance.

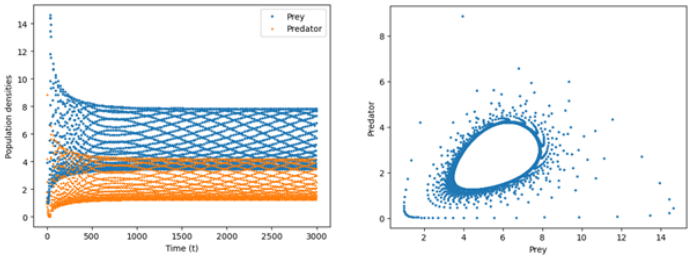

Figure 7: Simulation illustrating the system's (29) oscillation behavior with a large amplitude in prey and a small amplitude in predator for $b = 0.152$.

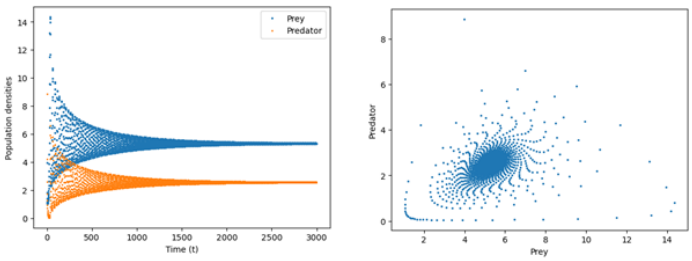

Figure 8: Simulation illustrating the system's (29) asymptotic stability behavior for $b = 0.0152$.

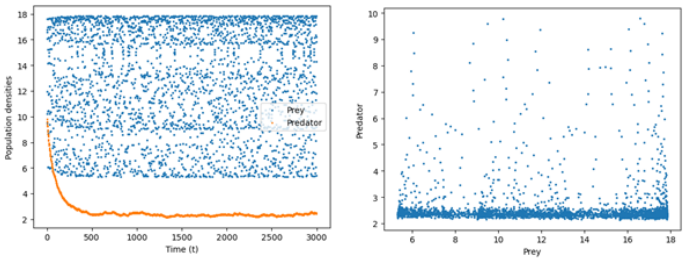

Figure 9: Simulation illustrating the chaotic behavior in the system for a specific set of parameters (for the values refer the text).

and analyze how the delay affects the system's stability. Numerical simulations of model (3) demonstrate that increasing the time delay can destabilize the positive equilibrium, leading to the emergence of a limit cycle through a Hopf bifurcation. Using normal for m theory and the center manifold theorem, we derive analytical expressions that characterize the direction and stability of the bifurcating periodic solutions. Our results show that bifurcation occurs when the delay parameter crosses a critical threshold. Biologically, the presence of a strong Allee effect significantly influences the system dynamics by destabilizing the coexistence equilibrium and altering conditions for population persistence. Likewise, temporal delays can disrupt steady predator–prey interactions and induce oscillatory or even chaotic behavior. The combined inclusion of delay and Allee effects enhances the biological realism of the model and provides deeper insights into complex interspecific interactions.

Furthermore, the discrete system (29) exhibits richer and more complex dynamics, including shifts from prey dominance to predator dominance, the emergence and disappearance of limit cycles as the prey survival rate varies, and the onset of chaotic behavior under certain parameter regimes. These findings underscore the crucial roles that Allee effects and time delays play in shaping ecological population dynamics.

9 Declarations

Funding

This research supported by National Natural Science Foundation of China (No. 62363005).

Competing Interests

The authors declare that there are no conflicts of interest related to this manuscript. No financial, personal, or professional relationships exist that could inappropriately influence, or be perceived to influence, the work presented in this paper within the past three years. Consequently, the publication of this manuscript will not be impeded by any conflicts of interest.

Ethical Approval

Not applicable.

Authors's Contributions

All authors contributed equally. All the authors read and approved the final manuscript.

Availability Data and Materials

No data was used for the research described in the article.

Acknowledgements

We sincerely thank the Department of Interdisciplinary Sciences at NIFTEM Knowledge Centre, Kundli, India, for their cooperation. The authors are thankful the editors and reviewers who have supported us in improving this manuscript.

References

[1] F. Courchamp, L. Berec, and J. Gascoigne, *Allee Effects in Ecology and Conservation*, Oxford Univ. Press, Oxford, UK, 2008.

[2] E. Gonzalez-Olivares and A. Rojas-Palma, Multiple limit cycles in a Gause-type predator–prey model with Holling type III functional response and Allee effect on prey, *Bull. Math. Biol.* **73** (2011), 1378–1397.

[3] F. Hilker, Population collapse to extinction: the catastrophic combination of parasitism and Allee effect, *J. Biol. Dyn.* **4** (2010), 86–100.

[4] F. Hilker, M. Langlais, and H. Malchow, The Allee effect and infectious diseases: extinction, multistability, and disappearance of oscillations, *Am. Nat.* **173** (2009), 72–88.

[5] A. Morozov, S. Petrovskii, and B. L. Li, Spatiotemporal complexity of patchy invasion in a predator–prey system with the Allee effect, *J. Theor. Biol.* **238** (2006), 18–35.

[6] P. J. Pal and T. Saha, Dynamical complexity of a ratio-dependent predator–prey model with strong additive Allee effect, *Appl. Math.* **146** (2015), 287–298.

[7] M. Sen and A. Morozov, Bifurcation analysis of a ratio-dependent prey–predator model with the Allee effect, *Ecol. Complex.* **11** (2012), 12–27.

[8] M. Wang and M. Kot, Speeds of invasion in a model with strong or weak Allee effects, *Math. Biosci.* **171** (2001), 83–97.

[9] S. R. Zhou, Y. F. Liu, and G. Wang, The stability of predator–prey systems subject to the Allee effects, *Theor. Popul. Biol.* **67** (2005), 23–31.

[10] L. Shi, H. Liu, Y. Wei, M. Ma, and J. Ye, The permanence and periodic solution of a competitive system with infinite delay, feedback control, and Allee effect, *Adv. Differ. Equ.* **2018** (2018), 400.

[11] H. Liu, Z. Li, M. Gao, H. Dai, and Z. Liu, Dynamics of a host–parasitoid model with Allee effect for the host and parasitoid aggregation, *Ecol. Complex.* **6** (2009), 337–345.

[12] J. Wang, J. Shi, and J. Wei, Predator–prey system with strong Allee effect in prey, *J. Math. Biol.* **62** (2011), 291–331.

[13] J. Wang, J. Shi, and J. Wei, Dynamics and pattern formation in a diffusive predator–prey system with strong Allee effect in prey, *J. Differ. Equ.* **251** (2011), 1276–1304.

[14] Y. Cai, C. Zhao, W. Wang, and J. Wang, Dynamics of a Leslie–Gower predator–prey model with additive Allee effect, *Appl. Math. Model.* **39** (2015), 2092–2106.

[15] C. Li and H. Zhu, Canard cycles for predator–prey systems with Holling types of functional response, *J. Differ. Equ.* **254** (2013), 879–910.

[16] Y. Li and D. Xiao, Bifurcations of a predator–prey system of Holling and Leslie types, *Chaos Solitons Fractals* **34** (2007), 606–620.

[17] Y. Qu and J. Wei, Bifurcation analysis in a time-delay model for prey–predator growth with stage-structure, *Nonlinear Dyn.* **49** (2007), 285–294.

[18] J. P. Tripathi, S. Tyagi, and S. Abbas, Global analysis of a delayed density-dependent predator–prey model with Crowley–Martin functional response, *Commun. Nonlinear Sci. Numer. Simul.* **30** (2016), 45–69.

[19] J. Ylikarjula, S. Alaja, J. Laakso, and D. Tesar, Effects of patch number and dispersal patterns on population dynamics and synchrony, *J. Theor. Biol.* **207** (2000), 377–387.

[20] X. Wang and J. Wei, Dynamics in a diffusive predator–prey system with strong Allee effect and Ivlev-type functional response, *J. Math. Anal. Appl.* **422** (2015), 1447–1462.

[21] Z. Ma, H. Tang, S. Wang, and T. Wang, Bifurcation of a predator–prey system with generation delay and habitat complexity, *J. Korean Math. Soc.* **55** (2018), 43–58.

[22] B. Dennis, Allee effects: population growth, critical density, and the chance of extinction, *Nat. Resour. Model.* **3** (1989), 481–538.

[23] M. A. Lewis and P. Kareiva, Allee dynamics and the spread of invading organisms, *Theor. Popul. Biol.* **43** (1993), 141–158.

[24] L. Berec, E. Angulo, and F. Courchamp, Multiple Allee effects and population management, *Trends Ecol. Evol.* **22** (2007), 185–191.

[25] F. Courchamp, T. Clutton-Brock, and B. Grenfell, Inverse density dependence and the Allee effect, *Trends Ecol. Evol.* **14** (1999), 405–410.

[26] P. A. Stephens and W. J. Sutherland, Consequences of the Allee effect for behaviour, ecology, and conservation, *Trends Ecol. Evol.* **14** (1999), 401–405.

[27] B. D. Hassard, N. D. Kazarinoff, and Y. H. Wan, *Theory and Application of Hopf Bifurcation*, Cambridge Univ. Press, Cambridge, 1981.

[28] C. Binaca, M. Ferrara, and L. Guerrini, The Cai model with time delay: existence of periodic solutions and asymptotic analysis, *Appl. Math. Inf. Sci.* **7** (2013), 21–27.

[29] X. Liu and D. Xiao, Complex dynamic behaviour of a discrete-time predator–prey system, *Chaos Solitons Fractals* **32** (2007), 80–94.

[30] R. Lopez-Ruiz and D. Fournier-Prunaret, Complex behaviour in a discrete coupled logistic model for the symbiotic interaction of two species, *Nonlinear Anal. Real World Appl.* (2004).

[31] A. E. Elsadany, H. A. El-Metawally, E. M. Elabbasy, and H. N. Agiza, Chaos and bifurcation of a nonlinear discrete prey–predator system, *Comput. Ecol. Softw.* **2** (2012), 169–180.

[32] A. E. Elsadany, Dynamical complexities in a discrete-time food chain, *Comput. Ecol. Softw.* **2** (2012), 124–139.

[33] H. Smith, *An Introduction to Delay Differential Equations with Applications to the Life Sciences*, Springer, 2011.

[34] Y. Kuang, *Delay Differential Equations with Applications in Population Dynamics*, Academic Press, 1993.

[35] S. Elaydi, *An Introduction to Difference Equations*, 3rd ed., Springer, 2005.

[36] R. E. Mickens, *Difference Equations: Theory and Applications*, Van Nostrand Reinhold, 1990.